Journal of Polyphenols
2025, 7 (3): 112–126
journal homepage: http://jpolyph.magtechjournal.com

Genistein solid dispersion: preparation, physical-chemical characters and anti-oxidant properties

Xiaofei Liu, Yang Liu, Hongyue Wang, Xiangrong Zhang *

Faculty of Function Food and Wine, Shenyang Pharmaceutical University, Shenyang 110016, China

Abstract The aim of this study was to enhance the applicability of genistein (GEN) and investigate genistein solid dispersion (GEN-SD). The optimal process parameters were determined as follows: anhydrous ethanol volume ratio of 4:1, ultrasonication time of 30 min, rotary evaporation temperature of 50 °C, and a drug-to-carrier mass ratio of 1:7. The results of the dissolution and solubility experiments showed that the dissolution rate and solubility of the optimized solid dispersion were significantly improved compared to pure GEN. Comprehensive characterization of the GEN-SD using X-ray diffraction, differential scanning calorimetry, scanning electron microscopy, and Fourier transform infrared spectroscopy clarified variations in crystalline form, thermal properties, and microscopic morphology. Antioxidant experiments showed that GEN-SD exhibited antioxidant activity and could effectively scavenge various free radicals. Stability studies demonstrated that GEN-SD was stable at a high temperature of 60 ℃ and a light intensity of 4500 lx.

Keywords: Genistein; Solid dispersion; Polyvinylpyrrolidone K30; Antioxidant

1 Introduction

Genistein (GEN) is an isoflavonoid compound that is widely distributed in leguminous plants, including soybean, fructus sophorae, lobed kudzuvine root and their products [1]. It is the major component of soy isoflavones [2, 3]. GEN powder is yellow in color with chemical name of 5,7,4'-trihydroxyisoflavone (Fig. 1), molecular formula is $C_{15}H_{10}O_5$ and molecular weight is 270.241 g/mol [4]. GEN has various biological activities, such as antibacterial, antioxidant, anti-inflammatory, and estrogen-like effects [1, 5, 6]. Genistein is non-toxic and has a wide range of potential applications in medicine, food and other fields [7]. Genistein can be used as a dietary supplement to protect neurons and prevent cognitive impairment [8, 9]. However, the low water solubility and bioavailability of GEN limit its applications [10, 11]. Some researchers have developed some formulation strategies to enhance solubility and bioavailability, including solid dispersions [12], microemulsions [13], complexes [14, 15] and other formulations.

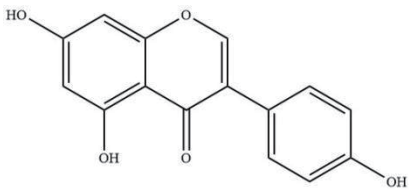

Fig. 1 Chemical structure of genistein

The solid dispersions (SD) are systems where a polymer matrix is used to disperse a desired hydrophobic compound in an amorphous/non-

* Corresponding authors: Xiangrong Zhang zhangxr@vip.sina.com.
These authors have no conflict of interest to declare.

equilibrium state to improves the water solubility and stability of an active ingredient [16, 17]. Deeksha Shukla [18] employed spray-drying technology to prepare ferulic acid-leucine solid dispersions for treatment chemotherapy-induced cognitive impairment (CICI). The enhanced bioavailability through the preparation of chrysin solid dispersions was studied by Chenhui Wang [19], demonstrating efficacy in amelioration of hyperlipidemia in rat models. Syed Assim Haq [20] developed andrographolide solid dispersions, to enhance the solubility and improve dissolution rate of the poorly soluble component. Among them, the solubilization mechanism of SD may be due to the reduction of particle size, the transformation of its crystalline structure and a significant improvement in wettability, which are all factors that work together to improve the solubility [21, 22].

Therefore, the aim of this study was to prepare genistein solid dispersion (GEN-SD) by solvent evaporation method and suitable carrier materials were screened by saturation solubility method [19]. The formulation was optimized using one factor and orthogonal experiments, and the optimal preparation was characterized, evaluated and compared with GEN active pharmaceutical ingredient (API) and physical mixtures (PM). The antioxidant activities and stability were also evaluated.

2 Materials and methods

2.1 Materials

Genistein (purity > 97%) was purchased from Shanghai Maclin Biochemical Technology Co., Ltd (Shanghai, China). PVP K30 was acquired from Tianjin Bodi Chemical Co., Ltd (Tianjin, China). Distilled water was acquired from Hangzhou Wahaha Group Co., Ltd (Hangzhou, China). Ethanol was obtained from Tianjin Lian Longbohua Pharmaceutical and Chemical Co., Ltd (Tianjin, China). 2,2-Diphenyl-1-picrylhydrazyl was purchased from Shanghai Maclin Biochemical Technology Co., Ltd (Shanghai, China). 2,2′-azinobis (3-ethylbenzothiazoline-6-sulphonate was purchased from Shanghai Yien Chemical Technology Co., Ltd (Shanghai, China). Hydroxyl radical scavenging assay kit was purchased from Nanjing Jiancheng Bioengineering Institute (Nanjing, China).

2.2 Selection of carriers

The carrier material for genistein solid dispersion (GEN-SD) was selected based on the solubilizing evaluation of polyvinylpyrrolidone K30 (PVP K30), polyethylene glycol 4000 (PEG 4000), sucrose, inulin, and citric acid (CA) on genistein [23]. Excess GEN-SD powder prepared from different carriers was dissolved in equal volume of distilled water respectively. Then it was placed in an air bath thermostatic shaker (Jiangsu, China) at 37 ℃ and shaken at 100 r/min for 48 h. After centrifugation and filtration through a 0.45 μm microporous filter membrane, a clarified GEN-SD solution was obtained. The absorbance was measured at a wavelength of 260 nm using a UV spectrophotometer (Shanghai, China), and equilibrium solubility at 48 h was calculated according to a pre-established standard curve. The standard curve of Genistein was linear in the range of 1-5 μg/mL (r = 0.9999).

2.3 Preparation of GEN-SD and GEN-PM

The solvent evaporation method was employed to prepare GEN-SD. A specific ratio of GEN was mixed with the carrier in ethanol solution. The clear solution of GEN was transferred to a rotary evaporator (Zhengzhou, China) to remove excess ethanol after homogeneous mixing via ultrasonication. The obtained GEN-SD was dried and pulverized.

Genistein physical mixture (GEN-PM) was prepared by the grinding method. GEN and the carrier were weighed in specific proportions, placed together in a mortar and pestle, and thoroughly mixed to obtain GEN-PM.

2.4 Molecular docking

The molecular docking simulations of genistein

with PVP K30 was performed to elucidate the intermolecular interaction mechanisms between the GEN and PVP K30 in GEN-SD. The lowest-energy conformation generated by the AutoDock 4.2.6 system was identified as the optimal binding conformation between genistein and PVP K30.

2.5 In vitro dissolution studies

The *in vitro* dissolution test was conducted in the dissolution medium of phosphate buffer (pH 6.8, 100 mL) at 37 ± 0.5 °C with an air bath thermostatic shaker at 100 rpm [24]. Each sample solution (5 mL) was collected at definite time of 5, 10, 20, 30, 40 and 60 min and filtered through 0.45 μm microporous membranes. The equal volumes of dissolution medium was added at the same temperature. The absorbance of the filtrate was measured by UV method to calculate dissolution at each time point.

2.6 Solubility test

The saturation solubility of GEN, GEN-PM and GEN-SD was studied. An excess of the sample was placed in a centrifuge tube, and the same volume of pH 6.8 phosphate buffer was added and mixed thoroughly, and shaken at 100 rpm for 48 h at 37 ℃ in an air bath thermostatic shaker to fully dissolve the sample [25]. The obtained solution was filtered through 0.45 μm microporous filter membrane and the absorbance of the subsequent filtrate was measured at 260 nm.

2.7 Characterization of GEN-SD

2.7.1 Scanning electron microscope (SEM)

Conformational characterization of GEN, PVP K30, GEN-PM and GEN-SD powder was carried out using scanning electron microscopy (Zeiss, Germany). The sample is uniformly adhered to the conductive adhesive to make the sample (ETH = 3kV), and the sample surface is sprayed with gold and then tested.

2.7.2 X-ray diffraction (XRD)

Crystalline characterization of GEN, PVP K30, GEN-PM and GEN-SD was carried out using X-ray diffractometer (Rigaku, Japan). All samples were placed in an X-ray diffractometer and scanned. The scanning conditions were: copper target, scanning range 5°-80°, test step size 0.02°, scanning speed 5°/min.

2.7.3 Thermogravimetric analysis (TGA) and differential scanning calorimetry (DSC)

The relationship between the properties and temperature of GEN, PVP K30, GEN-PM and GEN-SD was determined using TG-DSC simultaneous thermal analyzer (Netzsch, Germany). The samples were protected under a nitrogen atmosphere with a nitrogen flow rate of 50 mL/min. The samples were heated from 30 °C to 550 °C at a rate of 10 °C/min.

2.7.4 Fourier transform infraredspectroscopy (FT-IR)

Fourier transform infrared spectroscopy allows the study of the interaction between GEN and PVP K30. GEN, PVP K30, GEN-PM and GEN-SD sample powders were analyzed by Fourier transform infrared spectroscopy (Thermo Fisher, America). The samples were mixed with potassium bromide at a 1:200 ratio, ground, pressed into flakes, and placed in an infrared spectrometer for scanning within the wavenumber range of 4000-500 cm^{-1}.

2.8 Antioxidant studies

2.8.1 DPPH radical scavenging capacity

DPPH radical (2,2-Diphenyl-1-picrylhydrazyl) for evaluation of antioxidant level of GEN [26]. The DPPH ethanol solution, which exhibited a purple color, was mixed thoroughly with the sample. After reacting in the dark for 30 min, the UV absorbance of the mixture was measured at 517 nm. The following

formula was used to derive the DPPH radical scavenging rate of the samples:

$$\text{DPPH radical scavenging capacity} = [1 - (A_2 - A_1 / A_0)] \times 100\% \quad (1)$$

Where, A_0 is the absorbance of an equal amount of DPPH solution mixed with ethanol, A_1 is the absorbance of an equal amount of sample solution mixed with ethanol, A_2 is the absorbance of an equal amount of sample solution mixed with DPPH solution.

2.8.2 ABTS radical scavenging capacity

ABTS radical (2,2′-azinobis (3-ethylbenzothiazoline-6-sulphonate) is soluble in water and ethanol [27]. ABTS can produce blue-green free radicals, and the antioxidant capacity of a substance is judged by the change in UV absorbance. The ABTS radical cation solution was prepared by mixing equal volumes of ABTS aqueous solution (7 mM) and potassium persulfate solution (2.45 mM), followed by 12-hour incubation in the dark at 25 °C to allow complete oxidation. Appropriate amount of ethanol was used to dilute the ABTS base solution so that the absorbance at 734 nm was 0.70 ± 0.02, and the ABTS working solution was made. The ABTS working solution was mixed with the samples and left at room temperature away from light for 6 min and the absorbance was measured at 734 nm. The ABTS radical scavenging rate was derived using a calculation formula:

$$\text{ABTS radical scavenging capacity} = [1 - (A_1 - A_2 / A_0)] \times 100\ 100\% \quad (2)$$

Where, A_0 is the absorbance of ABTS working solution (3.9 mL) mixed with ethanol (0.1 mL), A_1 is the absorbance of ABTS working solution (3.9 mL) mixed with sample solution (0.1 mL), A_2 is the absorbance of ethanol (3.9 mL) mixed with sample solution (0.1 mL).

2.8.3 Hydroxyl radical scavenging capacity

The Fenton reaction is the most widely used chemical method for generating hydroxyl radicals (•OH) [28]. The amount of H_2O_2 is directly proportional to the quantity of •OH produced by the Fenton reaction. Upon coloration with Griess reagent, hydroxyl radicals form a violet-red product. The fading of this color after reaction with test compounds indicates antioxidant activity by scavenging the radicals.

In this assay, a commercially available hydroxyl radical scavenging assay kit was utilized to assess the antioxidant properties of genistein. Solution preparation and measurements were performed according to the manufacturer's instructions. The hydroxyl radical scavenging rate was calculated using the following formula:

$$\text{Hydroxyl radical scavenging} = (A_2 - A_3 / A_2 - A_1) \times 100\% \quad (3)$$

Where, A_1 is the absorbance of the blank group, A_2 is the absorbance of the control group, and A_3 is the absorbance of the test group.

2.9 Stability analysis

The stability of GEN and GEN-SD were evaluated by observing and recording the sample states, along with calculating the genistein content and retention rate, under three conditions: high temperature (60 ℃), high humidity (25 ℃, RH 92.5%/75%), and light exposure (25 ℃, 4500 lx). The formula for calculating the retention rate is as follows:

$$\text{Retention rate} = w_2 / w_1 \times 100\% \quad (4)$$

Here, w_2 is the content of the sample after storage and w_1 is the initial content of the sample.

2.9.1 High temperature stability

Appropriate amounts of GEN and GEN-SD were weighed into separate weighing flasks, evenly spread on the bottom to form a uniform layer with a thickness not exceeding 3 mm. The open weighing flasks were maintained at 60 °C, with samples

periodically collected at day 0, 5, and 10 to examine their appearance and content.

2.9.2 High humidity stability

Appropriate amounts of GEN and GEN-SD were weighed into separate weighing flasks, evenly spread on the bottom to form a uniform layer with a thickness not exceeding 3 mm. The open weighing flasks were stored in a desiccator at 25 ºC, RH 92.5% and RH 75% for ten days and samples were taken periodically on days 0, 5 and 10 to examine their appearance, content and hygroscopicity.

2.9.3 Light stability

Appropriate amounts of GEN and GEN-SD were weighed into separate weighing flasks, evenly spread on the bottom to form a uniform layer with a thickness not exceeding 3 mm. The weighing flasks were left open at a temperature of 25 ºC and a light intensity of 4500 lx for 10 days, and samples were taken periodically on days 0, 5, and 10 to examine their appearance and content.

2.10 Statistical analysis

All experiments were conducted in triplicate using a randomized design. Results are expressed as mean ± standard deviation (SD).

3 Results and discussion

3.1 Selection of carriers

The carrier was screened using saturated solubility of genistein (GEN) as the investigation index, and the results are shown in Fig. 2. Among them, polyvinylpyrrolidone K30 (PVP K30) demonstrated the best solubilizing effect with a saturated solubility of 61 μg/mL, which was superior to polyethylene glycol 4000 (PEG 4000), sucrose, inulin and citric acid (CA). Pre-tests confirmed that PVP K30 exhibited no inhibitory effect on genistein dissolution. According to the solubility and dissolution results, PVP K30 was selected as the carrier for the genistein solid dispersions (GEN-SD). PVP K30 is a water-soluble polymer with a high safety profile. It is often used as pharmaceutical excipient [29].

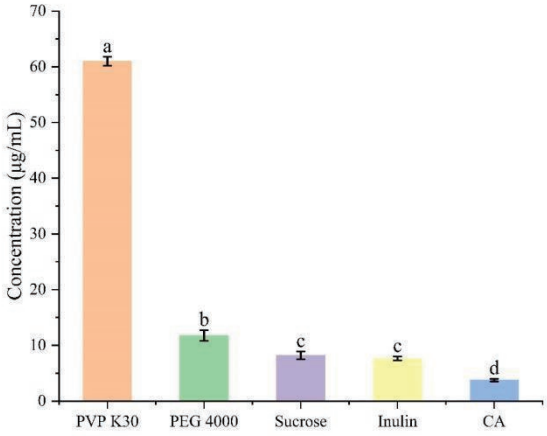

Fig. 2 Solubility of GEN in water using solid dispersions prepared from different carriers. Different letters indicate significant differences between values (One way ANOVA, $P < 0.05$)

3.2 Formulation and process optimization of genistein solid dispersions

Based on the process flow, it was hypothesized that the anhydrous ethanol volume ratio (2:1, 4:1, 6:1), ultrasonication time (15 min, 30 min, 45 min), drug-to-carrier mass ratio (1:5, 1:7, 1:9), and rotary evaporation temperature (30 ℃, 40 ℃, and 50 ℃) might have an effect on the preparation process and the final dissolution results of the solid dispersions

(Table 1). Therefore, these four factors were selected as experimental variables. The cumulative dissolution percentage at 60 min served as the evaluation index, and the optimal prescription was screened through orthogonal test.

The results are shown in Table 2. Although the dissolution of solid dispersions was higher at a drug-to-carrier ratio of 1:9, excessive PVP K30 dosage can lead to increased formulation costs, result in excessively low drug loading capacity and high viscosity, which is unfavorable for the preparation of subsequent dosage forms. Based on the combined results of the above investigations, the optimal prescription of GEN-SD was determined as anhydrous ethanol volume ratio of 4:1; sonication time of 30 min; rotary evaporation temperature of 50 ℃; and drug-to-carrier ratio of 1:7.

Table 1 Factor and level of orthogonal experiment

Level	Factor			
	A	B	C	D
	Anhydrous ethanol volume ratio	Ultrasonication time	Rotary evaporation temperature	Drug-to-carrier mass ratio
1	2:1	15 min	30 ℃	1:5
2	4:1	30 min	40 ℃	1:7
3	6:1	45 min	50 ℃	1:9

Table 2 $L_9(3^4)$ Orthogonal experimental design and the results

No.	Factor				Cumulative dissolution in 60 min (%)
	A	B	C	D	
1	3	2	3	1	73.54
2	3	3	1	2	71.92
3	2	1	3	2	76.85
4	2	3	2	1	73.23
5	2	2	1	3	75.19
6	1	3	3	3	76.54
7	1	1	1	1	66.04
8	3	1	2	3	73.46
9	1	2	2	2	76.12
K_1	72.90	72.18	71.05	70.94	
K_2	75.09	74.95	74.27	74.96	
K_3	73.03	73.90	75.64	75.05	
R	2.19	2.77	4.59	4.11	
Prioritize factors	C>D>B>A				
Best combination	$A_2 B_2 C_3 D_3$				

3.3 Molecular docking

The molecular docking results showed that strong hydrogen bonds were formed between the 5-hydroxyl and 7-hydroxyl oxygen atoms of GEN and the carbonyl oxygen atoms in the PVP K30 polymer chain (bond lengths: 2.1-2.2 Å), with a binding free energy (ΔG) of -5.37 kcal/mol (Fig. 3A). The binding free energy (ΔG) can be used to evaluate the strength of interactions between molecules and polymers. Generally, a stable system has a ΔG value less than -5 kcal/mol. This indicates a strong binding tendency between GEN and PVP K30. The carbonyl groups in PVP K30 specifically bind to the hydroxyl groups of GEN through intermolecular hydrogen bonds, thereby significantly improving GEN stability and solubility.

3.4 In vitro dissolution studies

The dissolution curves are shown in Fig. 3B. The cumulative dissolution of both GEN and GEN-PM did not reach 50.00%. However, after the preparation of GEN-SD, the cumulative dissolution reached 88.73%, indicating a significant improvement in dissolution performance. Typically, grinding reduces the particle size of GEN and increases the contact area. Thus, physical mixtures may also slightly enhance GEN dissolution [30, 31]. The GEN-SD dissolution curves were fitted and the best fit model was found to be first-order (Table 3).

Table 3 Fitting of dissolution curves for GEN-SD

Model	Equation	R^2
Zero-order kinetic	$y = 73.05 + 0.40x$	0.1933
First-order kinetic	$y = 87.96\ (1\text{-}e^{-0.37x})$	0.9587
Higuchi	$y = 4.42x^{1/2} + 61.91$	0.3673
Ritger-peppas	$y = 58.23x^{0.12}$	0.5328

3.5 Solubility test

The saturation solubility results are displayed in Fig. 3C. The solubility of GEN and GEN-PM are lower than that of GEN-SD. The solubility of GEN-SD is 465 times higher than that of GEN. This enhancement may be attributed to the uniform dispersion and amorphous-state saturation of genistein within PVP K30, combined with the uniform particle size and strong wettability of the prepared GEN-SD [32, 33], thereby increasing the solubility of genistein.

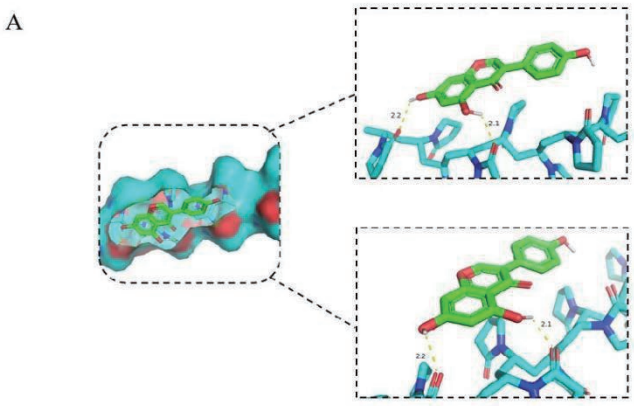

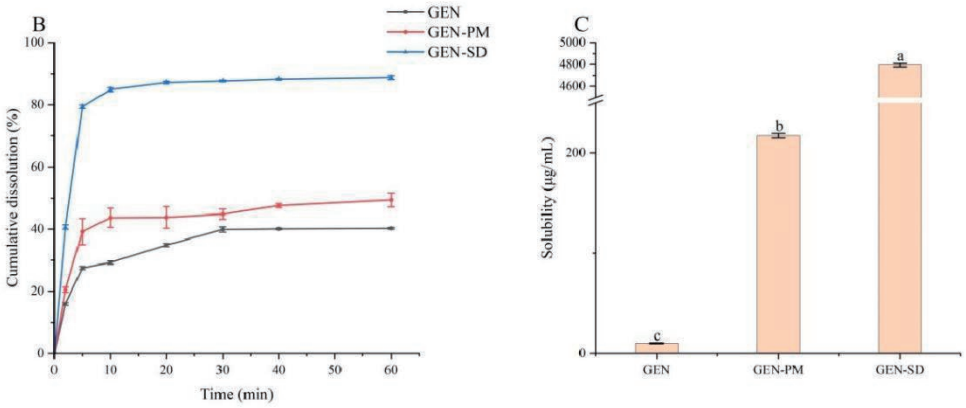

Fig. 3 A: The optimal conformation formed through molecular docking between genistein and PVP K30. B: Dissolution curves and C: solubility of GEN, GEN-PM, and GEN-SD. Different letters indicate significant differences between values (One way ANOVA, $P < 0.05$)

3.6 Characterization of GEN-SD

3.6.1 Scanning electron microscope (SEM)

The results are shown in Fig. 4. Scanning electron microscopy allows observation of the morphological characteristics of GEN, PVP K30, GEN-PM and GEN-SD. GEN exhibits a rod-shaped crystal structure. The carrier PVP K30 appears as spherical pellets with smooth surface, some of which are dented. The crystal structure of genistein and the spherical structure of PVP K30 remain visible in GEN-PM, indicating that GEN and PVP K30 are simply physically mixed. GEN-SD displays an irregular, sharp-edged lamellar structure, and the characteristic structures of both PVP K30 and GEN disappear. This demonstrates that genistein is dispersed into PVP K30 in an amorphous manner.

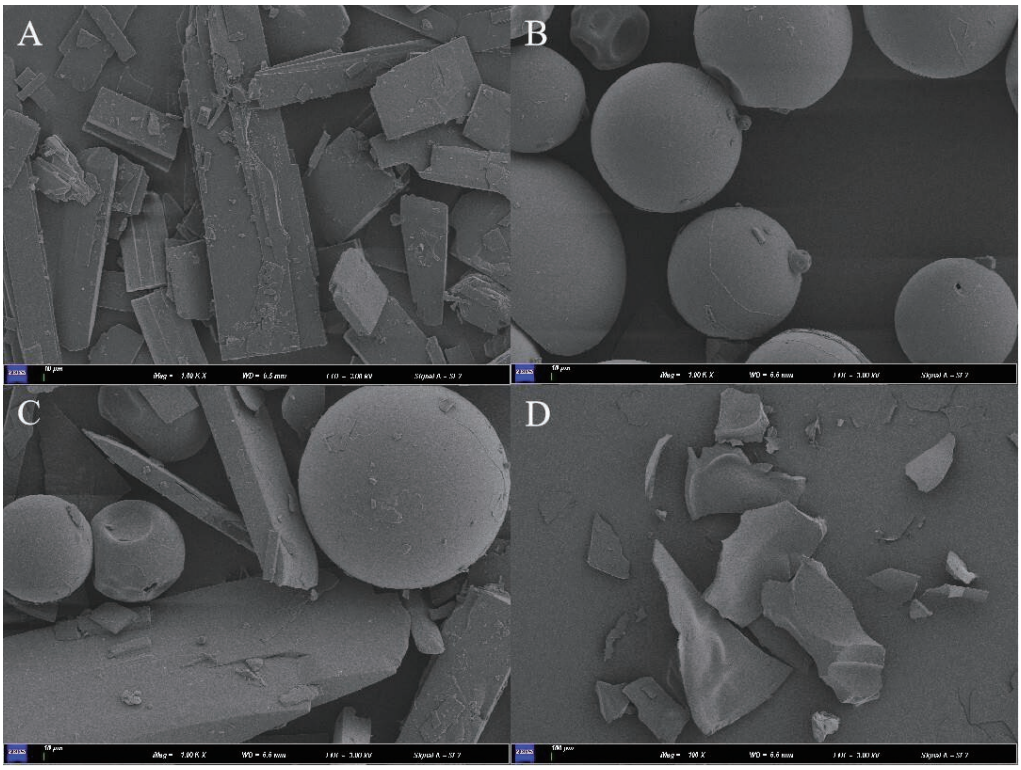

Fig. 4 SEM images of A: GEN (1.00 KX), B: PVP K30 (1.00 KX), C: GEN-PM (1.00 KX), D: GEN-SD (100 X)

3.6.2 X-ray diffraction (XRD)

The XRD results of the samples are shown in Fig. 5A. GEN exhibited multiple distinct crystal diffraction peaks, indicating its well-crystallized nature. The weak intensity of PVP K30's XRD peaks confirms its amorphous characteristic. The XRD pattern of the GEN-PM demonstrates a superposition of GEN and PVP K30 diffraction peaks, and the crystal peaks of genistein were clearly observed, but with reduced intensity. In contrast, the XRD pattern of GEN-SD reveals the complete disappearance of all genistein-related crystal peaks. These results confirm that GEN is molecularly dispersed within the PVP K30 carrier in an amorphous state, consequently exhibiting enhanced solubility [34].

3.6.3 Thermogravimetric analysis (TGA) and differential scanning calorimetry (DSC)

The TG and DTG curves of GEN, PVP K30, GEN-PM and GEN-SD are shown in Fig. 5B. The DTG curve of GEN did not show significant changed in the initial stage, whereas PVP K30, GEN-PM, and GEN-SD exhibited weak peaks at 65 °C. The TG curves indicated minimal mass loss for these three samples, likely attributed to the hygroscopic nature of PVP K30 in air, where the presence of PVP K30 caused dehydration reactions [35]. As the temperature gradually increased, the samples began to decompose progressively. Significant endothermic peaks were observed for GEN, PVP K30, GEN-PM, and GEN-SD at 347.9 °C, 433.0 °C, 432.3 °C, and 434.9 °C, respectively. The TG curves indicated that at 550 °C, the mass losses of these samples were 65.17%, 82.13%, 70.56%, and 78.26%, which could be attributed to thermal decomposition. The crystalline structure of GEN contributed to its enhanced stability, resulting in the lowest mass loss. GEN-PM retained the crystalline structure of GEN due to the simple mixing of GEN and PVP K30, exhibited lower mass loss compared to PVP K30 and GEN-SD. Although genistein in the solid dispersion existed in an amorphous state, it still exhibits higher thermal stability than the water-soluble PVP K30, resulting in slightly lower mass loss compared to PVP K30.

The DSC curves of the samples are shown in Fig. 5C. GEN displays a sharp endothermic peak at 301.2 °C due to its crystal structure [36]. PVP K30 exhibits a faint broad peak at 67.5 °C. The DSC curve of the GEN-PM contains endothermic peak at 301.2 °C for genistein, albeit with reduced intensity. Notably, no genistein endothermic peak is observed in the DSC curve of GEN-SD, indicating the transition of genistein from a crystalline to an amorphous state. These findings are consistent with the XRD results.

3.6.4 Fourier transform infrared spectroscopy (FT-IR)

The results are shown in Fig. 5D. The O-H and C=O stretching vibration peaks of GEN appear at wavenumbers 3411 cm^{-1} and 1650 cm^{-1}, respectively [12, 37, 38]. The C-H and C=O stretching vibration peaks of PVP K30 are observed at wavenumbers 2973 cm^{-1} and 1652 cm^{-1} [39, 40]. The infrared spectrum of the GEN-PM exhibits characteristic stretching vibration peaks of both GEN and PVP K30, indicating that they had no chemical interactions, but rather a physical mixture. In contrast, in the GEN-SD, the O-H stretching vibration peak at 3411 cm^{-1} of GEN was weakened, broadened and red-shifted to 3436 cm^{-1}, accompanied by diminished or absent characteristic PVP K30 peaks. The reason may be that the functional groups in genistein react with PVP K30 and hydrogen bonds are formed between the GEN and PVP K30 [41].

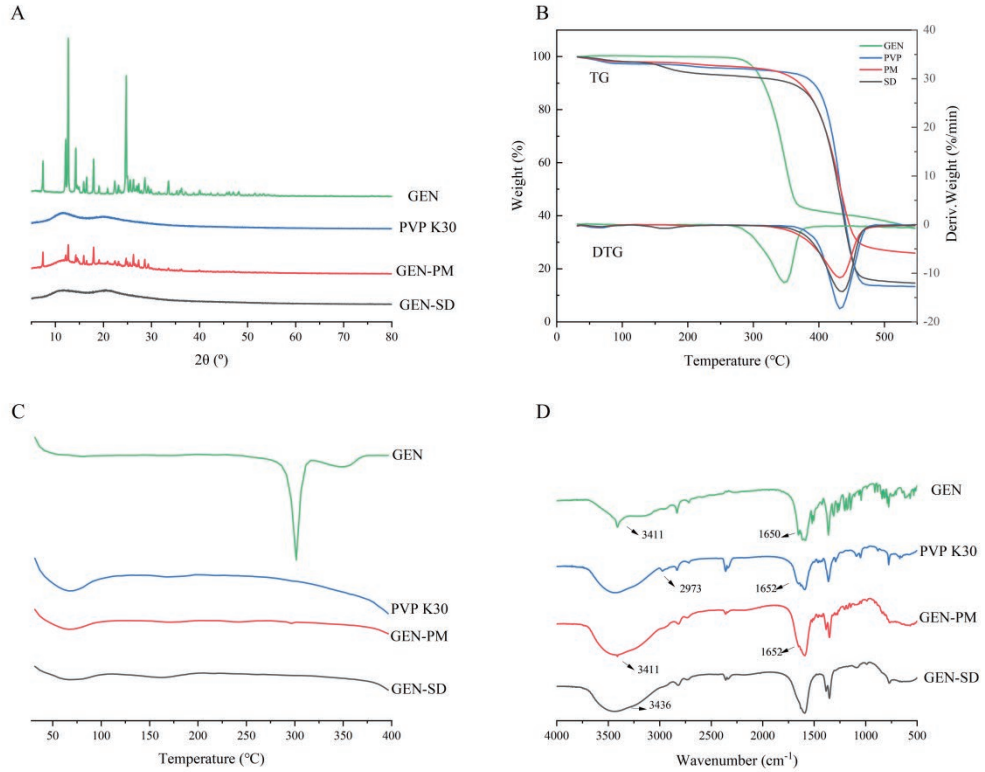

Fig. 5 A: XRD patterns, B: TG and DTG curves, C: DSC curves, D: FT-IR spectra of GEN, PVP K30, GEN-PM, and GEN-SD

3.7 Antioxidant studies

3.7.1 DPPH radical scavenging capacity

The DPPH radical scavenging results are shown in Fig. 6A. Ascorbic acid (VC) was more effective in scavenging DPPH radicals than GEN and GEN-SD at concentrations between 1.5 mg/mL and 7.5 mg/mL. With the gradual increase in concentration, the DPPH radical scavenging rate of GEN-SD increased from 25.2% to 75.1% (IC_{50} = 3.454 mg/mL), which was significantly higher than that of GEN. PVP K30 has no antioxidant activity. Thus, the increase in antioxidant effect may be due to the transformation of GEN into an amorphous state, which increases the contact area with the oxides and improves the solubilization of GEN.

3.7.2 ABTS radical scavenging capacity

The ABTS radical scavenging results are shown in Fig. 6B. The antioxidant capacity of both genistein and solid dispersions was lower than that of VC at the same concentration. PVP K30 had no antioxidant effect. The ABTS radical scavenging rate of GEN reached 52.1% at a concentration of 1.2 mg/mL with a more moderate increase. The ABTS radical scavenging rate of GEN-SD increased from 35.3% to 64.1% (IC_{50} = 0.579 mg/mL). It was shown that the preparation as solid dispersions could improve the antioxidant capacity of genistein. By comparing the ABTS and DPPH radical scavenging tests, it could be found that the ABTS method is more sensitive than the DPPH method. It is possible that the spatial blockage of the DPPH radical site makes it more difficult for the substances to capture the free radicals, making it necessary to select a higher concentration of substances for the DPPH antioxidant assay [42].

3.7.3 Hydroxyl radical scavenging capacity

Fig. 6C displays the hydroxyl radical scavenging results. PVP K30 exhibited no significant antioxidant activity. The hydroxyl radical scavenging rates of GEN, GEN-SD, and the positive control (VC) all

increased progressively with concentration, yet their antioxidant activities remained lower than that of VC. Specifically, the scavenging rate of genistein rose from 33.15% to 75.7%, while that of the GEN-SD increased from 34.9% to 80.4% (IC_{50} = 0.29 mg/mL), indicating enhanced antioxidant capacity compared to pure GEN. These findings align with the results from DPPH and ABTS antioxidant assays, demonstrating that formulating genistein into a solid dispersion effectively improves its antioxidant activity.

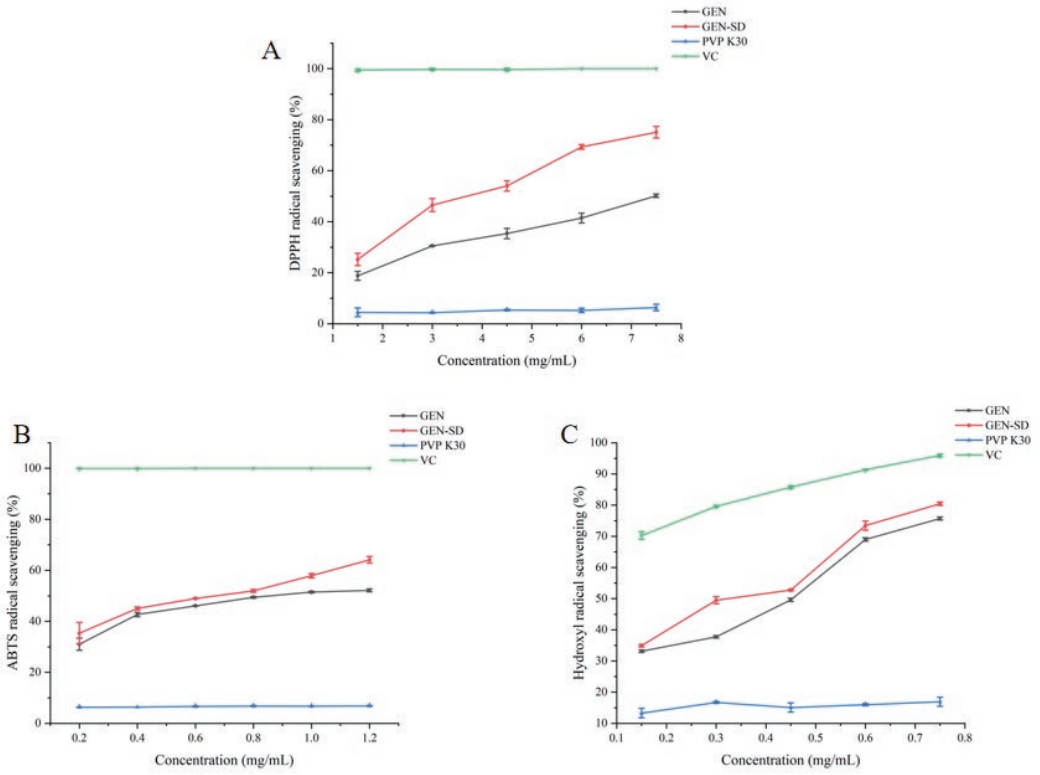

Fig. 6 A: DPPH radical, B: ABTS radical, C: hydroxyl radical scavenging activity of different concentrations of GEN, GEN-SD, PVP K30, VC

3.8 Stability analysis

3.8.1 High temperature stability

As shown in Fig. 7, no significant changes in the appearance of GEN were observed after 10 days at 60 ℃. However, according to Table 4, it could be seen that GEN was unstable at high temperatures, with the retention rate decreases gradually, and the final retention rate on the 10th day was only 82.48%. The appearance of the GEN-SD became darker after 10 days, probably due to the recrystallization of a small portion of genistein [43]. The retention rate of GEN-SD was 93.93% on day 10 (Table 5), which was significantly higher than that of GEN. Thus, it was demonstrated that the preparation of GEN-SD could improve the stability of genistein at high temperatures.

3.8.2 High humidity stability

GEN did not show significant changes after 10 days at 92.5% RH (Fig. 7). However, there was a significant change in the properties of GEN-SD. The GEN-SD changed from light yellow powder to a light yellow, transparent, sticky liquid, and increased weight. GEN-SD had low genistein content due to high moisture content, which may be attributed to the excessive moisture absorption of PVP K30 (Table 5). The results of GEN-SD after 10 days of storage at 75% RH are shown in Fig. 7 and Table 5. A small

amount of agglomeration was observed in the GEN-SD. The retention rate of GEN-SD was 91.15%, which was higher than that of GEN, indicating that there was a better protection of genistein when prepared as solid dispersions. Since GEN-SD are sensitive to high humidity, the GEN-SD should be stored in a dry place under seal [35].

3.8.3 Light stability

As shown in Fig. 7, there was no significant change in the properties of both GEN and GEN-SD after 10 days of storage at 4500 lx light intensity. The retention rate of GEN decreased to 84.89% on day 10, indicating that GEN is more sensitive to light and therefore needs to be stored in dark conditions (Table 4). The retention rate of GEN-SD after 10 days of storage was 92.27%, which was significantly higher than that of GEN (Table 5). It indicates that the GEN-SD is more stable under light exposure. The improved stability may be attributed to the encapsulating effect of the solid dispersion preparation on GEN, which prevents direct exposure to intense light [44, 45].

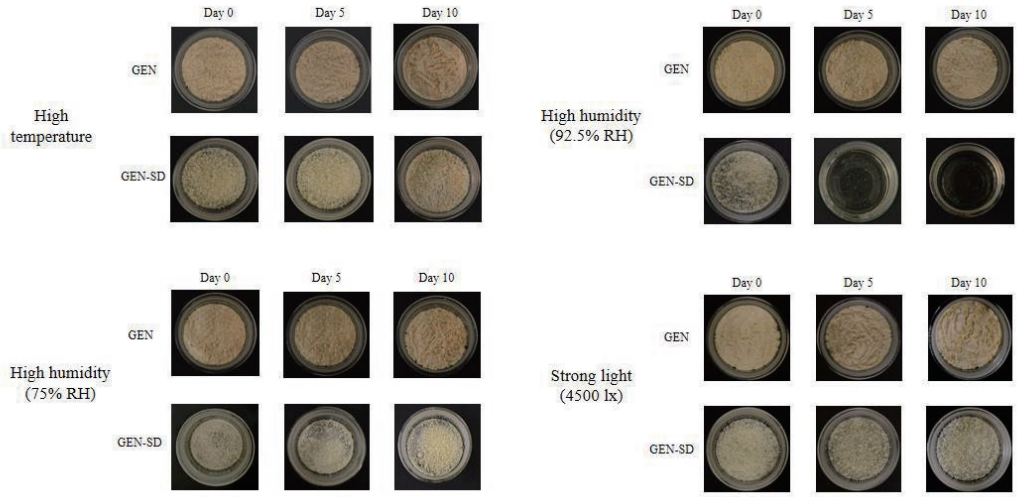

Fig. 7 Stability of GEN and GEN-SD stored for 10 days

Table 4 Stability of GEN exposed to high temperature, high humidity and strong light

Index	Time (d)	Content (%)	Retention rate (%)	Hygroscopicity (%)	Appearance
High temperature (60 ℃)	0	98.18 ± 0.73	100.00	\	Yellow powder
	5	85.51 ± 2.57	87.10 ± 3.16	\	Yellow powder
	10	80.98 ± 0.65	82.48 ± 1.08	\	Yellow powder
High humidity (92.5% RH)	0	99.32 ± 0.18	100.00	0	Light yellow powder
	5	92.09 ± 1.29	92.72 ± 1.46	0	Light yellow powder
	10	86.75 ± 1.22	87.34 ± 1.10	0	Yellow powder
High humidity (75% RH)	0	99.32 ± 0.18	100.00	0	Yellow powder
	5	87.82 ± 0.89	88.43 ± 1.00	0	Yellow powder
	10	86.59 ± 2.39	87.18 ± 2.24	0	Yellow powder
Strong light (4500 lx)	0	98.56 ± 0.56	100.00	\	Yellow powder
	5	87.77 ± 2.29	89.05 ± 2.14	\	Yellow powder
	10	83.56 ± 1.59	84.89 ± 1.49	\	Yellow powder

Table 5 Stability of GEN-SD exposed to high temperature, high humidity and strong light

Index	Time (d)	Content (%)	Retention rate (%)	Hygroscopicity (%)	Appearance
High temperature	0	12.36 ± 0.05	100.00	\	Light yellow powder
	5	11.63 ± 0.02	94.09 ± 0.30	\	Light yellow powder
	10	11.61 ± 0.09	93.93 ± 0.96	\	Yellow powder
High humidity (92.5% RH)	0	12.39 ± 0.04	100.00	0	Light yellow powder
	5	9.24 ± 0.21	74.6 ± 1.87	27.50	Light yellow transparent viscous liquid
	10	9.22 ± 0.08	74.44 ± 0.85	27.50	Light yellow transparent viscous liquid
High humidity (75% RH)	0	12.39 ± 0.04	100.00	0	Light yellow powder
	5	12.24 ± 0.02	98.82 ± 0.40	7.50	Light yellow powder
	10	11.29 ± 0.02	91.15 ± 0.44	7.50	Light yellow powder
Strong light (4500 lx)	0	12.37 ± 0.03	100.00	\	Light yellow powder
	5	11.58 ± 0.13	93.67 ± 1.30	\	Light yellow powder
	10	11.41 ± 0.14	92.27 ± 1.33	\	Light yellow powder

4 Conclusion

In this study, PVP K30 was the matrix for preparation of GEN-SD. Dissolution and solubility experiments showed that GEN-SD performed well in these two aspects, with significant improvement compared to GEN. The characterization and properties were clarified by SEM, XRD, DSC, FT-IR, which further revealed the intrinsic mechanism of the performance enhancement. The results of antioxidant experiments showed that the GEN-SD not only possessed good antioxidant ability, but also demonstrated significant inhibition of specific bacterial species. Stability studies indicate that it maintains stable performance under high-temperature and light conditions, but requires avoidance of high-humidity environments. Through this study provides theoretical support for the further development and application of GEN. However, the toxicity, safety and bioactivity of genistein solid dispersion need to be evaluated in the future time.

Acknowledgement

This study was supported by department of Education of Liaoning Province (Natural Science, Strategic Industrialization Project (LJ212410163061).

References

[1] Sharifi-Rad J, Quispe C, Imran M, et al. Genistein: An Integrative Overview of Its Mode of Action, Pharmacological Properties, and Health Benefits [J]. Oxid Med Cell Longev, 2021, 2021: 3268136.

[2] Bernatoniene J, Kazlauskaite JA, Kopustinskiene DM. Pleiotropic Effects of Isoflavones in Inflammation and Chronic Degenerative Diseases [J]. Int J Mol Sci, 2021, 22 (11): 5656.

[3] Panche AN, Diwan AD, Chandra SR. Flavonoids: an overview [J]. J Nutr Sci, 2016, 5: e47.

[4] Goh YX, Jalil J, Lam KW, et al. Genistein: A Review on its Anti-Inflammatory Properties [J]. Front Pharmacol, 2022, 13: 820969.

[5] Mei J, Chen X, Liu J, et al. A Biotransformation Process for Production of Genistein from Sophoricoside by a Strain of Rhizopus oryza [J]. Sci Rep, 2019, 9 (1): 6564.

[6] Jeong JW, Lee HH, Han MH, et al. Anti-inflammatory effects of genistein via suppression of the toll-like receptor 4-mediated signaling pathway in lipopolysaccharide-stimulated BV2 microglia [J]. Chem Biol Interact, 2014, 212: 30-39.

[7] Michael McClain R, Wolz E, Davidovich A, et al. Genetic toxicity studies with genistein [J]. Food Chem Toxicol, 2006, 44 (1): 42-55.

[8] Liu Q, Zhang R, Chen Y, et al. Dietary Flavonoid Intake and Risk of Mild Cognitive Impairment in the Elderly: A Case-Control Study [J]. Nutr Metab Insights, 2024, 17: 11786388241283779.

[9] Ronchetti S, Labombarda F, Del Core J, et al. The phytoestrogen genistein improves hippocampal neurogenesis and cognitive impairment and decreases neuroinflammation in an animal model of metabolic syndrome [J]. J Neuroendocrinol, 2025, 37 (2): e13480.

[10] Jaiswal KS, Malka O, Shauloff N, et al. Genistein carbon dots exhibit antioxidant and anti-inflammatory effects in vitro [J]. Colloids Surf B Biointerfaces, 2023, 223: 113173.

[11] Tang H, Wang S, Li X, et al. Prospects of and limitations to the clinical applications of genistein [J]. Discov Med, 2019, 27 (149): 177-188.

[12] Qiu C, Zhang Y, Fan Y, et al. Solid Dispersions of Genistein via Solvent Rotary Evaporation for Improving Solubility, Bioavailability, and Amelioration Effect in HFD-Induced Obesity Mice [J]. Pharmaceutics, 2024, 16 (3): 306.

[13] Vu QL, Fang CW, Suhail M, et al. Enhancement of the Topical Bioavailability and Skin Whitening Effect of Genistein by Using Microemulsions as Drug Delivery Carriers [J]. Pharmaceuticals (Basel), 2021, 14 (12): 1233.

[14] Shete VS, Telange DR, Mahajan NM, et al. Development of phospholipon®90H complex nanocarrier with enhanced oral bioavailability and anti-inflammatory potential of genistein [J]. Drug Deliv, 2023, 30 (1): 2162158.

[15] Shao Y, Zhao XX, Guo M, et al. Delivery Mechanism of the Pharmaceutical Complex of Genistein-Adenine Based on Spectroscopic and Molecular Modelling at Atomic Scale [J]. Chem Biodivers, 2021, 18 (2): e2000944.

[16] Vo CL, Park C and Lee BJ. Current trends and future perspectives of solid dispersions containing poorly water-soluble drugs [J]. Eur J Pharm Biopharm, 2013, 85 (3 Pt B): 799-813.

[17] Baghel S, Cathcart H, O'Reilly NJ. Polymeric Amorphous Solid Dispersions: A Review of Amorphization, Crystallization, Stabilization, Solid-State Characterization, and Aqueous Solubilization of Biopharmaceutical Classification System Class II Drugs [J]. J Pharm Sci, 2016, 105 (9): 2527-2544.

[18] Shukla D, Kaur S, Singh A, et al. Enhanced antichemobrain activity of amino acid assisted ferulic acid solid dispersion in adult zebrafish (Danio rerio) [J]. Drug Deliv Transl Res, 2024, 14 (12): 3422-3437.

[19] Wang C, Liu X, Zhao R, et al. The Amorphous Solid Dispersion of Chrysin in Plasdone(®) S630 Demonstrates Improved Oral Bioavailability and Antihyperlipidemic Performance in Rats [J]. Pharmaceutics, 2023, 15 (10): 2378.

[20] Assim Haq S, Paudwal G, Banjare N, et al. Sustained release polymer and surfactant based solid dispersion of andrographolide exhibited improved solubility, dissolution, pharmacokinetics, and pharmacological activity [J]. Int J Pharm, 2024, 651: 123786.

[21] Hiew TN, Solomos MA, Kafle P, et al. The importance of surface composition and wettability on the dissolution performance of high drug loading amorphous dispersion formulations [J]. J Pharm Sci, 2025, 114 (1): 289-303.

[22] Huang H, Zhang Y, Hu C. Study on the crystallinity of PEG on the crystalline size of flavonoids in a crystalline dispersion system [J]. Eur J Pharm Biopharm, 2024, 205: 114536.

[23] Liang H, Sun C, Feng Z, et al. Study on Integrated Pharmacokinetics of the Component-Based Chinese Medicine of Ginkgo biloba Leaves Based on Nanocrystalline Solid Dispersion Technology [J]. Int J Nanomedicine, 2022, 17: 4039-4057.

[24] Ye Q, Li T, Li J, et al. Development and evaluation of tea polyphenols loaded water in oil emulsion with zein as stabilizer [J]. J Drug Delivery Sci Tech, 2020, 56: 101528.

[25] Li S, Zhang Z, Gu W, et al. Hot Melt Extruded High-Dose Amorphous Solid Dispersions Containing Lumefantrine and Soluplus [J]. Int J Pharm, 2024, 665: 124676.

[26] Zhu J, Xu Z, Liu X. Chemical composition, antioxidant activities, and enzyme inhibitory effects of Lespedeza bicolour Turcz. essential oil [J]. J Enzyme Inhib Med Chem, 2025, 40 (1): 2460053.

[27] Zhang T, Wang H, Hu H, et al. Composite film based on carboxymethyl cellulose and gellan gum with honokiol-β-cyclodextrin inclusion complex: Characterization and application in strawberry preservation [J]. Int J Biol Macromol, 2024, 282 (Pt 1): 136740.

[28] Shimada O, Yasuda H. Hydroxyl radical scavenging action of tinoridine [J]. Agents Actions, 1986, 19 (3-4): 208-214.

[29] Kurakula M, Rao G. Pharmaceutical assessment

of polyvinylpyrrolidone (PVP): As excipient from conventional to controlled delivery systems with a spotlight on COVID-19 inhibition [J]. J Drug Deliv Sci Technol, 2020, 60: 102046.

[30] Markeev VB, Tishkov SV, Vorobei AM, et al. Modeling of the Aqueous Solubility of N-butyl-N-methyl-1-phenylpyrrolo[1,2-a] pyrazine-3-carboxamide: From Micronization to Creation of Amorphous-Crystalline Composites with a Polymer [J]. Polymers (Basel), 2023, 15 (20): 4136.

[31] Gera T, Nagy E, Smausz T, et al. Application of pulsed laser ablation (PLA) for the size reduction of non-steroidal anti-inflammatory drugs (NSAIDs) [J]. Sci Rep, 2020, 10 (1): 15806.

[32] Ishtiaq M, Manzoor H, Khan IU, et al. Curcumin-loaded soluplus® based ternary solid dispersions with enhanced solubility, dissolution and antibacterial, antioxidant, anti-inflammatory activities [J]. Heliyon, 2024, 10 (14): e34636.

[33] Li Y, Wei Q, Su J, et al. Encapsulation of astaxanthin in OSA-starch based amorphous solid dispersions with HPMCAS-HF/Soluplus® as effective recrystallization inhibitor [J]. Int J Biol Macromol, 2024, 279 (Pt 1): 135421.

[34] Khuanekkaphan M, Netsomboon K, Fristiohady A, et al. Development of Quercetin Solid Dispersion-Loaded Dissolving Microneedles and In Vitro Investigation of Their Anti-Melanoma Activities [J]. Pharmaceutics, 2024, 16 (10): 1276.

[35] Zhou Z, Chen J, Zhang ZX, et al. Solubilization of luteolin in PVP40 solid dispersion improves inflammation-induced insulin resistance in mice [J]. Eur J Pharm Sci, 2022, 174: 106188.

[36] Jangid AK, Solanki R, Patel S, et al. Genistein encapsulated inulin-stearic acid bioconjugate nanoparticles: Formulation development, characterization and anticancer activity [J]. Int J Biol Macromol, 2022, 206: 213-221.

[37] Bian Q, Liu J, Tian J, et al. Binding of genistein to human serum albumin demonstrated using tryptophan fluorescence quenching [J]. Int J Biol Macromol, 2004, 34 (5): 333-337.

[38] Abdelwahab HE, Elhag M, El Sadek MM. Removal of As(V) and Cr(VI) using quinoxaline chitosan schiff base: synthesis, characterization and adsorption mechanism [J]. BMC Chem, 2024, 18 (1): 225.

[39] El-Aassar MR, Ibrahim OM, Fouda MMG, et al. Wound dressing of chitosan-based-crosslinked gelatin/ polyvinyl pyrrolidone embedded silver nanoparticles, for targeting multidrug resistance microbes [J]. Carbohydr Polym, 2021, 255: 117484.

[40] Rosiak N, Tykarska E, Miklaszewski A, et al. Enhancing the Solubility and Dissolution of Apigenin: Solid Dispersions Approach [J]. Int J Mol Sci, 2025, 26 (2): 566.

[41] Su D, Bai M, Wei C, et al. Combining solubilization and controlled release strategies to prepare pH-sensitive solid dispersion loaded with albendazole: in vitro and in vivo studies [J]. Front Vet Sci, 2024, 11: 1522856.

[42] Rumpf J, Burger R, Schulze M. Statistical evaluation of DPPH, ABTS, FRAP, and Folin-Ciocalteu assays to assess the antioxidant capacity of lignins [J]. Int J Biol Macromol, 2023, 233: 123470.

[43] Martynek D, Ridvan L, Sivén M, et al. Stability and recrystallization of amorphous solid dispersions prepared by hot-melt extrusion and spray drying [J]. Int J Pharm, 2025, 672: 125331.

[44] Coelho L, Almeida IF, Sousa Lobo JM, et al. Photostabilization strategies of photosensitive drugs [J]. Int J Pharm, 2018, 541 (1-2): 19-25.

[45] Serajuddin AT. Solid dispersion of poorly water-soluble drugs: early promises, subsequent problems, and recent breakthroughs [J]. J Pharm Sci, 1999, 88 (10): 1058-1066.